

Matched filter in the low-number count Poisson noise regime: an efficient and effective implementation

R. Vio¹ and P. Andreani²

¹ Chip Computers Consulting s.r.l., Viale Don L. Sturzo 82, S.Liberale di Marcon, 30020 Venice, Italy
e-mail: robertovio@tin.it,

² ESO, Karl Schwarzschild strasse 2, 85748 Garching, Germany
e-mail: pandrean@eso.org

Received; accepted

ABSTRACT

The matched filter (MF) is widely used to detect signals hidden within the noise. If the noise is Gaussian, its performances are well-known and describable in an elegant analytical form. The treatment of non-Gaussian noises is often cumbersome as in most of the cases there is no analytical framework. This is true also for Poisson noise which, especially in the low-number count regime, presents the additional difficulty to be discrete. For this reason, in the past methods based on heuristic or semi-heuristic arguments have been proposed. Recently, an analytical form of the MF has been obtained but in the proposed implementation the computation of the probability of false detection or false alarm (PFA) is based on numerical simulations. This is an inefficient and time consuming approach. Here, we present an effective method to compute the PFA based on the saddlepoint approximation which is fast, able to provide excellent results and easy to implement. Theoretical arguments are provided as well the results of some numerical experiments.

Key words. Methods: data analysis – Methods: statistical

1. Introduction

Detecting signals embedded in noise is a common issue in many research and engineering areas. In the case of Gaussian noise, the matched filter (MF) represents a standard tool (Tuzlukov 2001; Minkof 2002; Osche 2002; Briggs 2004; Levy 2008; Yao et al. 2013). This is because according to the Neyman-Pearson theorem, it provides the greatest probability of true detection subject to a constant probability of false detection (e.g. see Kay 1998). In non-Gaussian case, however, the MF is more difficult to obtain and, even if available, more difficult to use. In particular the computation of the probability of false detection or false alarm (PFA) may be complex. In Astronomy, this case may happen in the search for high-energy point sources where the noise is Poissonian (i.e. non-additive) and consists, together with the signal of interest, only in a few counts per pixels. For this reason, in the past alternative procedures based on heuristic or semi-heuristic arguments have been preferred (Stewart 2006, and reference therein). In a recent work, Ofek & Zackay (2017) provide an analytical form of the MF but the computation of the PFA is based on numerical simulations. Such an approach lacks flexibility and it is time consuming. In the present paper we propose a method to compute the PFA based on the technique of the saddlepoint approximation which is very fast, flexible and able to provide accurate results.

In Sect. 2 the problem of the detection of a signal in Poisson noise is formalized whereas the saddlepoint approximation method is described in Sect. 3 and its application illustrated in Sect. 4. The results of a few numerical experiments are given in Sects. 5-6 and some comments concerning the use in practical applications in Sect. 7. Finally, the conclusions are given in Sect. 8.

2. The mathematics of the problem

In this section the basic properties of the MF in the case of Poisson noise are described. For ease of presentation, arguments will be developed using a one-dimensional formalism. In the case of higher-dimensional situations, the coordinate system has to be intended as multi-dimensional¹.

To illustrate the procedure for the detection of a deterministic and discrete signal of known structure $s = [s(0), s(1), \dots, s(N-1)]^T$, with length N , and the symbol T denoting a vector or matrix transpose, we assume the following:

- The searched signal takes the form $s = ag$ with a a positive scalar quantity (amplitude) and g typically a smooth function often somehow normalized (e.g., $\sum_{i=0}^{N-1} g(i) = 1$);
- The signal s is contaminated by a Poisson noise, i.e. the observed signal x is given by $x = \mathcal{P}(s + \lambda)$. Here, λ represents the intensity parameter of the noise background and $\mathcal{P}(\mu)$ denotes a Poisson random vector with independent entries and mean μ ;
- Although it is not a necessary condition in what follows, in the rest of the paper the parameter λ is assumed to be constant across x .

Under these conditions, the detection problem consists of deciding whether $x = n = \mathcal{P}(\lambda)$, i.e. it is pure noise (hypothesis H_0), or if it contains a contribution from a signal s (hypothesis H_1). In

¹ In the case of a two-dimensional map X , a one-dimensional signal x is obtained through $x = \text{VEC}[X]$, with $\text{VEC}[\cdot]$ the operator that transforms a matrix into a column array by stacking its columns one underneath the other.

this way, it is equivalent to a decision problem between the two hypotheses

$$\begin{cases} \mathcal{H}_0 : & \mathbf{x} = \mathcal{P}(\lambda); \\ \mathcal{H}_1 : & \mathbf{x} = \mathcal{P}(s + \lambda). \end{cases} \quad (1)$$

Under \mathcal{H}_0 the probability density function (PDF) of \mathbf{x} is given by $p(\mathbf{x}|\mathcal{H}_0)$ whereas under \mathcal{H}_1 by $p(\mathbf{x}|\mathcal{H}_1)$. Deciding between these two alternatives requires to fix the criterion to use for the detection. A common and effective criterion is the Neyman-Pearson criterion which consists in the maximization of the probability of detection PD under the constraint that the probability of false alarm PFA (i.e., the probability of a false detection) does not exceed a fixed value α . The Neyman-Pearson theorem (e.g., see Kay 1998) is a powerful tool which allows to design a decision process that pursues this aim: to maximize PD for a given PFA = α , decide \mathcal{H}_1 if the likelihood ratio

$$L(\mathbf{x}) = \frac{p(\mathbf{x}|\mathcal{H}_1)}{p(\mathbf{x}|\mathcal{H}_0)} > \gamma, \quad (2)$$

where the threshold γ is found from

$$\text{PFA} = \int_{\{\mathbf{x}: L(\mathbf{x}) > \gamma\}} p(\mathbf{x}|\mathcal{H}_0) d\mathbf{x} = \alpha. \quad (3)$$

In a recent work Ofek & Zackay (2017) show that criteria (2) and (3) lead to the test

$$T(\mathbf{x}) = \mathbf{x}^T \mathbf{f} > \gamma, \quad (4)$$

where

$$\mathbf{f} = \ln \left(1 + \frac{s}{\lambda} \right). \quad (5)$$

In practice, the test consists in filtering the signal \mathbf{x} with \mathbf{f} (i.e. the matched filter) and checking if the statistic $T(\mathbf{x})$ exceeds the threshold γ . From Eq. (5) it appears that the form of \mathbf{f} depends on the signal s . Here, an issue occurs due to the fact that in many practical applications (e.g. detection of point-sources in sky maps) only the template \mathbf{g} of the signal is known but not its amplitude a . The consequence of using the MF with an incorrect amplitude a is to reduce, for a fixed value of the PFA, the PD, i.e. to render the MF sub-optimal. In any case, Ofek & Zackay (2017) have shown that the results provided by the MF are not very sensitive to the precise value of a (see also below). This is not surprising given the logarithmic dependence of \mathbf{f} on λ . However, even for a specific value of a , the PDF of $T(\mathbf{x})$ under the hypothesis \mathcal{H}_0 is not available in analytical form. The reason is that, although $T(\mathbf{x})$ is given by a linear composition of Poisson random variables, its PDF is not Poissonian. This does not allow to fix the threshold γ corresponding to a prefixed value α of the PFA. The above mentioned authors bypass this problem by means of an approach based on numerical simulations. Such method, however, is not flexible and time consuming.

An alternative to the numerical simulations is the approximation of the unavailable PDF of $T(\mathbf{x})$ by some other PDF. For example, in the situations of high-number count noise regime, the Gaussian PDF may be a satisfactory choice. The same does not hold in the low-number count regime. In this case the saddlepoint approximation represents an effective solution.

3. Saddlepoint approximation basics

The saddlepoint approximation is a powerful tool able to provide accurate expressions of the PDFs and the corresponding cumulative distribution functions (CDF) which are not available in analytical form. Its derivation is rather technical. For this reason, here we present only the material useful for practical applications and refer to the monograph by Butler (2007) for the technical details.

The saddle point approximations of the PDF $f(x)$ and the CDF $F(x)$ of a continuous random variable X are given, respectively, by

$$\hat{f}(x) = \frac{1}{\sqrt{2\pi K''(\hat{\delta})}} \exp(K(\hat{\delta}) - \hat{\delta}x), \quad (6)$$

and

$$\hat{F}(x) = \begin{cases} \Phi(\hat{w}) + \frac{\phi(\hat{w})}{6\sqrt{2\pi F''(0)^{3/2}}} (1/\hat{w} - 1/\hat{u}) & \text{if } x \neq \mu, \\ \frac{1}{2} + \frac{K'''(0)}{6\sqrt{2\pi F''(0)^{3/2}}} & \text{if } x = \mu. \end{cases} \quad (7)$$

Here, $K(s)$ is the cumulant generating function (CGF) of $f(x)$,

$$K(s) = \ln(M(s)), \quad (8)$$

with

$$M(s) = \int_{-\infty}^{+\infty} f(x) e^{sx} dx \quad (9)$$

the corresponding moment generating function (MGF), and $\hat{\delta}$ the unique solution to the equation ²

$$K'(\hat{\delta}) = x, \quad (10)$$

with symbol “ ’ ” denoting derivative with respect s . Moreover, $\phi(y)$ and $\Phi(y)$ represent the standard Gaussian PDF and CDF, respectively, whereas \hat{w} and \hat{u} are given by

$$\hat{w} = \text{sign}(\hat{\delta}) \sqrt{2[\hat{\delta}x - K(\hat{\delta})]}, \quad (11)$$

with $\text{sign}(y)$ providing the sign of y , and

$$\hat{u} = \hat{\delta} \sqrt{K''(\hat{\delta})}. \quad (12)$$

To notice that $\hat{f}(x)$ will not, in general, integrate to one, although it will usually not be far off. Therefore, it has to be numerically normalized. Moreover, when ³ $x = E[X] = \mu$, the computation of $\hat{F}(x)$ is tricky since in this case $K'(0) = E[X]$ and then the solution of Eq. (10) becomes $\hat{\delta} = 0$. As a consequence, it happens that $K(0) = 0$ and accordingly, since from Eq. (11) it results $\hat{w} = 0$, the first equation in the system (7) becomes useless. This is the reason for the second equation in the system (11). For practical use, however, it is numerically more advantageous to use a linear interpolation based on the saddlepoint approximation to $E[X] \pm \epsilon$, where ϵ is chosen small enough to ensure high accuracy, but large enough to ensure numerical stability.

In the case X is a discrete random variable, the same equations hold with x substituted by k , which takes values in the set of the integer numbers, and keeping in mind that $1 - \hat{F}(k)$ provides the probability that $X \geq k$. Although the expressions Eqs. (6) and (7) are computable for any value of x whether real or integer-valued, $\hat{f}(k)$ and $\hat{F}(k)$ are meaningful approximations of $f(k)$ and $F(k)$ only for integer-valued arguments.

² Function $K(s)$ is always a strictly convex function when evaluated over the converge interval U of $M(s)$. Consequently, the mapping $K'(s)$ for $s \in U$ into the support of the PDF $f(x)$ is a bijection and thereof $K'(s)$ is strictly increasing (see pag. 6 in Butler 2007).

³ $E[\cdot]$ denotes the expectation operator.

4. Signal detection in the Poisson noise regime

The saddlepoint approximation to the PDF and the CDF of $T(\mathbf{x})$ in the Poisson case can be easily computed. Indeed, under the hypothesis \mathcal{H}_0 , $T(\mathbf{x})$ is given by a linear combination of Poisson random variables X with common parameter λ ,

$$T(\mathbf{x}) = y = \sum_{i=0}^{N-1} \hat{f}_i x_i. \quad (13)$$

Hence, its CGF $K(s)$ is given by

$$K(s) = \lambda \sum_{i=0}^{N-1} (e^{\hat{f}_i s} - 1), \quad (14)$$

with $s \in (-\infty, +\infty)$. It is trivial to see that its j -th derivative $K^{(j)}(s)$ is given by

$$K^{(j)}(s) = \lambda \sum_{i=0}^{N-1} \hat{f}_i^j e^{\hat{f}_i s}. \quad (15)$$

In order to be used in Eqs (6) and (7), these functions have to be computed at \hat{s} . This step requires the numerical solution of Eq. (10) that, however, does not present particular difficulties given that $K'(s)$ is an increasing function for $s \in (-\infty, +\infty)$. The only point to remember is that, since Eq. (10) cannot be solved when $x = 0$, $\hat{f}(x)$ is defined only for $x > 0$. However, it is easy to realize that for $X = 0$ it is $\hat{f}(0) = \exp(-\lambda N)$. This last is an exact result not only an approximation.

When using the saddlepoint approximation in the present context, it is necessary to consider that the PDF of $T(\mathbf{x})$ is of discrete type but it is not defined on a lattice (i.e. y does not take values on a regular grid of numbers). The point is that the arguments presented above hold only for integer values of k or, with minor modifications, when k takes values on a regular grid of numbers. However, except for extremely small values of λ , this PDF can be considered ‘‘almost continuous’’. Indeed, from combinatorial arguments it can be realized that, already for λ as small as 0.01 and \mathbf{f} given by a circular Gaussian with standard deviation $\sigma = 2$ pixels, the number of different values that y can take is of order of several thousands. In any case, there is considerable empirical evidence that saddlepoint methods are useful and maintain most of their accuracy even with discrete PDF not defined on a lattice (cf. pag. 27 in Butler 2007). The numerical simulations presented below confirm this result.

5. Some numerical experiments

Figure 1 compares the histogram $H(y)$ with the saddle point approximation $\hat{f}(y)$ (normalized to unit area) of the PDF $f(y)$ of the statistic $T(\mathbf{x})$ for the central pixel of a set of 10^5 MF filtered random realizations of a Poisson 13×13 pixels noise process. Four values of the parameter λ , say 0.01, 0.025, 0.05, and 0.1 (units in counts pix^{-1}), have been considered. The MF has been computed assuming s as a circular Gaussian with standard deviation $\sigma = 2$ pixels normalized to unit volume. For comparison, the Gaussian best fits $\phi(y)$ are also shown. From these figures it is visible that better results are obtainable increasing the values of λ . This is not an unexpected result since small values of λ imply most of the pixels with zero counts, a few with counts equal to one and very few with greater counts. Especially for ‘‘narrow’’ signals s , the consequence is a rough PDF for the statistic $T(\mathbf{x})$. However, in the case of $\lambda = 0.01$, the top-right panel of Fig. 1

shows that, although the saddlepoint approximation is not able to reproduce all the details of the $H(y)$, it provides a good envelope. As a result, a good approximation of the corresponding CDF can be obtained. This is supported by Fig. 2 which compares the sample CDF $\tilde{F}(y)$ with the $\hat{F}(y)$ corresponding to the PDFs in Fig. 1. The agreement is excellent. This is more evident in Fig. 3 where the relative errors $(\hat{F}(y) - \tilde{F}(y))/\tilde{F}(y)$ are plotted versus $\tilde{F}(y)$ for values of y such as $\tilde{F}(y) > 0.7$. This is an useful fact since in signal detection problems it is the complementary CDF $1 - F(y)$ and not the PDF $f(y)$ which does matter.

With very small values of λ the saddlepoint approximation does not work. However, it is questionable that in situations of very low-number count regime the MF could be an useful approach. For example, in the case of a 1000×1000 pixels map and $\lambda = 0.001$, only $N_0 = 1000$ pixels are expected with values greater than zero, i.e. only one pixel in each area of 30×30 squared pixels. Under these conditions the use of the MF does not make sense since there is nothing to filter. Moreover, the expected noise background should consist of 1000 bumps all with the same shape and amplitude. A more effective approach is based on the observation that the probability to have two counts in a pixel is of order of 5×10^{-7} . Thereof, all the non-zero pixels are expected to have one count. In addition, given that the probability of two pixels to occupy adjacent positions is of order of $4N_0/N_{\text{pix}}$, only four of them are expected to be bordering. In other words, the detection of a signal can be claimed with high confidence in presence of pixels with counts greater than one and possibly contiguous with other non-zero pixels.

The conclusion that can be drawn from these experiments is that the saddlepoint approximation is able to provide excellent results in situations of low levels of the noise background. As visible in Figs. 1-3, this is not true for the Gaussian approximation. Hence, to test if after the MF filtering the value y of a pixels is not due only to the noise, it is sufficient to check if $1 - \hat{F}(y) < \alpha$ with α a prefixed PFA.

6. MF vs the point spread function

In the case of Gaussian noise \mathbf{n} with covariance matrix \mathbf{C} , the MF can also be derived as the filter that maximizes the signal-to-noise ratio (SNR)⁴ or, in other words, the filter which provides the greatest amplification of the signal with respect to the noise. Such maximization can be obtained through the minimization of the variance of the filtered noise $\hat{\mathbf{f}}^T \mathbf{n}$ with the constraint that $\hat{\mathbf{f}}^T \mathbf{s} = a$ (i.e. filter $\hat{\mathbf{f}}$ does not modify the amplitude of the signal). Since the variance of the filtered noise is given by

$$\text{E}[(\hat{\mathbf{f}}^T \mathbf{n})(\hat{\mathbf{f}}^T \mathbf{n})] = \hat{\mathbf{f}}^T \text{E}[\mathbf{n}\mathbf{n}^T] \hat{\mathbf{f}} = \hat{\mathbf{f}}^T \mathbf{C} \hat{\mathbf{f}}, \quad (16)$$

the optimization model is⁵

$$\hat{\mathbf{f}}_{\text{SNR}} = \arg \min_{\hat{\mathbf{f}}} [\hat{\mathbf{f}}^T \mathbf{C} \hat{\mathbf{f}} - \tau (\hat{\mathbf{f}}^T \mathbf{s} - a)] \quad (17)$$

with τ a Lagrange multiplier. It can be shown that

$$\hat{\mathbf{f}}_{\text{SNR}} = \frac{\mathbf{C}^{-1} \mathbf{g}}{\mathbf{g}^T \mathbf{C}^{-1} \mathbf{g}}. \quad (18)$$

If the noise is stationary and of white-type, then $\hat{\mathbf{f}}_{\text{SNR}} \propto \mathbf{g}$. This means that, up to a constant factor, the MF coincides with the

⁴ Here, the quantity SNR is defined as the ratio between the squared amplitude of the filtered signal with the variance of the filtered noise.

⁵ We recall that the functions $\arg \min F(x)$ and $\arg \max F(x)$ provide the values of x of for which the function $F(x)$ has the smallest and greatest value, respectively.

template \mathbf{g} . As a consequence, in various astronomical applications (e.g. the detection of point-sources in two-dimensional maps) the MF coincides with the point spread function (PSF).

In the Poisson noise regime, this argument cannot be directly applied. The point is that, under the conditions we are working with, the noise level is constant across the background area but it changes in correspondence to the signal area. However, since the MF is often used in situations where the amplitude of the signal is smaller than the level of the noise, in first approximation it can be assumed that $s + \lambda \approx \lambda$. Therefore, the noise can be considered of additive type with a constant level everywhere. Hence, there are situations where \mathbf{g} can be an acceptable approximation of the MF. This conclusion is confirmed by Fig. 4 where the performance of the MF is compared with that of \mathbf{g} for various combinations of λ and a . In the experiments \mathbf{g} is a circular Gaussian with $\sigma = 2$ pixels, and the completeness has been estimated on the basis of 10^4 simulated 13×13 pixels maps.

A point to stress, however, is that in these simulations the true values of a have been used in the computation of the MF. For this reason, another set of numerical experiments similar to the previous one have been carried out but using an incorrect signal amplitude a^* . The results are shown in Figs. 5-7 for $a^* = 0.1, 10,$ and 100 . The indication that comes out from these figures is that, for a given value of λ , the performances of the MF effectively do not critically depend on the exact value of a . Only values of a^* very different from the true one determine an appreciable degradation of the results. Moreover, it appears less harmful to use values of a^* greater, rather than smaller, than the true value. The reason of this fact can be deduced from Fig. 8 which show the 1-D cut of the MF for different combinations of λ and a . With λ fixed, it is evident that when a increases the filtering action of the MF is stronger. This results in over-filtered signal but also in a more robust attenuation of the noise. On the contrary, using an a^* smaller than a will result in an insufficiently filtered noise. The former situation appears preferable.

7. The Saddlepoint approximation in practical applications

Although the arguments presented above indicate that the saddlepoint approximation is able to provide excellent results, we have to add some comments. In particular, it is important to point out that the MF (5) has been obtained under the assumption that the observed signal \mathbf{x} and the template \mathbf{s} have the same length N . This assumption implies that the position of \mathbf{s} within \mathbf{x} is known. In real situations this condition is rarely met. The standard procedure is to cross-correlate a map with the MF and to apply the detection test to the resulting most prominent peaks. However, as shown in Vio & Andreani (2016) and Vio et al. (2017) for the Gaussian case, the PDF $\psi(z)$ of the peaks $\{z\}$ of a random field is different from that of its generic points. Of course, the same holds also for the Poisson case. This is shown by Fig. 9 where the PDF $\hat{f}(y)$ of a 2000×2000 pixels Poisson random field with $\lambda = 0.1$ and filtered by means of the MF in Eq. (5) with \mathbf{s} a circular Gaussian with $\sigma = 2$ pixels, is compared with the histogram $H(z)$ of its peaks. It is evident that working with the peaks, and assuming the PDF $\hat{f}(y)$ for the the statistic $T(z)$ in Eq. (13), may severely underestimate the PFA with the risk to give statistical significance to features that belong to the noise.

Contrary to the Gaussian noise (Cheng & Schwartzman 2015a,b), the PDF of the peaks is not available for the Poissonian noise. Without it, a precise computation of the PFA is not possible. Moreover, there is the additional difficulty that, if N_p

peaks are present in a MF filtered map, then a number $\alpha \times N_p$ among them is expected to exceed by chance the prefixed detection threshold. For example, if $N_p = 1000$, then there is a high probability that a detection with a nominal PFA equal to 10^{-3} is spurious. Hence, the true PFA has to depend on N_p (look-elsewhere effect). The popular way-out to get around this issue is to assume $f(y)$ as PDF of the peaks (i.e. the peaks are regarded as generic points of the random field) and then to set $\text{PFA} = \alpha/N^*$ with N^* the number of independent pixels. If noise is colored, as it happens after the filtering operation, pixels are correlated one with each other. Therefore, N^* typically is smaller than N and has to be estimated. Usually the estimation of N^* is based on the correlation length of the signal. The rational is that pixels with a mutual distance wider than the correlation length can be considered independent. For instance, in the case of a two-dimensional map and a MF given by a circular Gaussian function with dispersion σ , Ofek & Zackay (2017) suggest that $N^* \approx N/\sigma^2$. This is to point out that such approach provides results which are only correct as an order of magnitude but no alternative is available if additional a priori information is missing.

In the present context, such procedure can be efficiently implemented by means of the order statistics, in particular by exploiting the statistical characteristics of the greatest value of a finite sample of identical and independently distributed (iid) random variable from a given PDF (Hogg et al. 2013). Under the iid condition, the PDF $p(y_{\max})$ and the CDF $P(y_{\max})$ of the greatest value among a set of N^* independent pixels with PDF $\hat{f}(y)$ are given by

$$p(y_{\max}) = N^* \left[\hat{F}(y_{\max}) \right]^{N^*-1} \hat{f}(y_{\max}), \quad (19)$$

and

$$P(y_{\max}) = \left[\hat{F}(y_{\max}) \right]^{N^*}, \quad (20)$$

respectively. Hence, by assuming that $z_{\max} = y_{\max}$ (the greatest value among a set of pixels coincides with that of a peak) a detection can be claimed when for a given peak it is $1 - P(y_{\max}) < \alpha$. This is an alternative, though equivalent, way to threshold the data which does not require the inversion of $P(y_{\max})$ to fix the parameter γ corresponding to a given α . In Vio et al. (2017) the quantity $1 - P(y_{\max})$ is called specific probability of false alarm (SPFA). The PDF $p(y_{\max})$ for the numerical experiment of this section is also shown in Fig. 9 as well the SPFA corresponding to the largest peak observed in the map. We stress that in the case of large maps, an alternative based on numerical simulation is not viable.

8. Conclusions

In this paper an efficient and effective implementation of the matched filter (MF) in the case of low-number count Poisson noise regime has been presented. In particular, it has been shown that, although the PDF and the CDF of the pixels counts after the MF filtering is not available, this can be approximated with excellent results by means of the saddlepoint approximation. With such a techniques it is possible to obtain a more accurate estimate of the probability of false detection or false alarm (PFA) without resorting to empirical or numerical methods.

References

Briggs, J. 2004, Target Detection by Marine Radar (London: IET)

- Butler, R.W. 2007, Saddlepoint Approximations with Applications (Cambridge: Cambridge University Press)
- Cheng, D., & Schwartzman, A. 2015a, *Extremes*, 18, 213
- Cheng, D., & Schwartzman, A. 2015b, arXiv:1503.01328 [math.PR]
- Hogg, R.V., McKean, J.W., & Craig, A.T. 2013, *Introduction to Mathematical Statistics* (New York: Pearson)
- Kay, S.M. 1998, *Fundamentals of Statistical Signal Processing: Detection Theory* (London: Prentice Hall)
- Levy, B.C. 2008, *Principles of Signal Detection and Parameter Estimation* (New York: Springer Science + Business Media)
- Macmillan, N.A., & Creelman, C.D. 2005, *Detection Theory: a User's Guide* (Mahwah: Lawrence Erlbaum Associates)
- Minkof, J. 2002, *Signal processing fundamentals and applications for communications and sensing* (Boston: Artech House)
- Ofek, E.O., & Zakay, B. 2017, arXiv:1709.01524 (*submitted to ApJ*)
- Osche, g.R. 2002, *Optical Detection Theory For Laser Applications* (Oboken: Wiley-Interscience)
- Stewart, I.M 2066, *A&A*, 454, 1009
- Tuzlukov, V.P. 2001, *Signal Detection Theory* (New York: Springer Science + Business Media)
- Vio, R., & Andreani, P. 2016, *A&A*, 589, A20
- Vio, R., Vergès, C., & Andreani, P. 2017, *A&A*, 604, A115
- Yao, K., Lorenzelli, F., & Chen, C.E. 2013, *Detection and Estimation for Communication and Radar Systems* (Cambridge: Cambridge University Press)

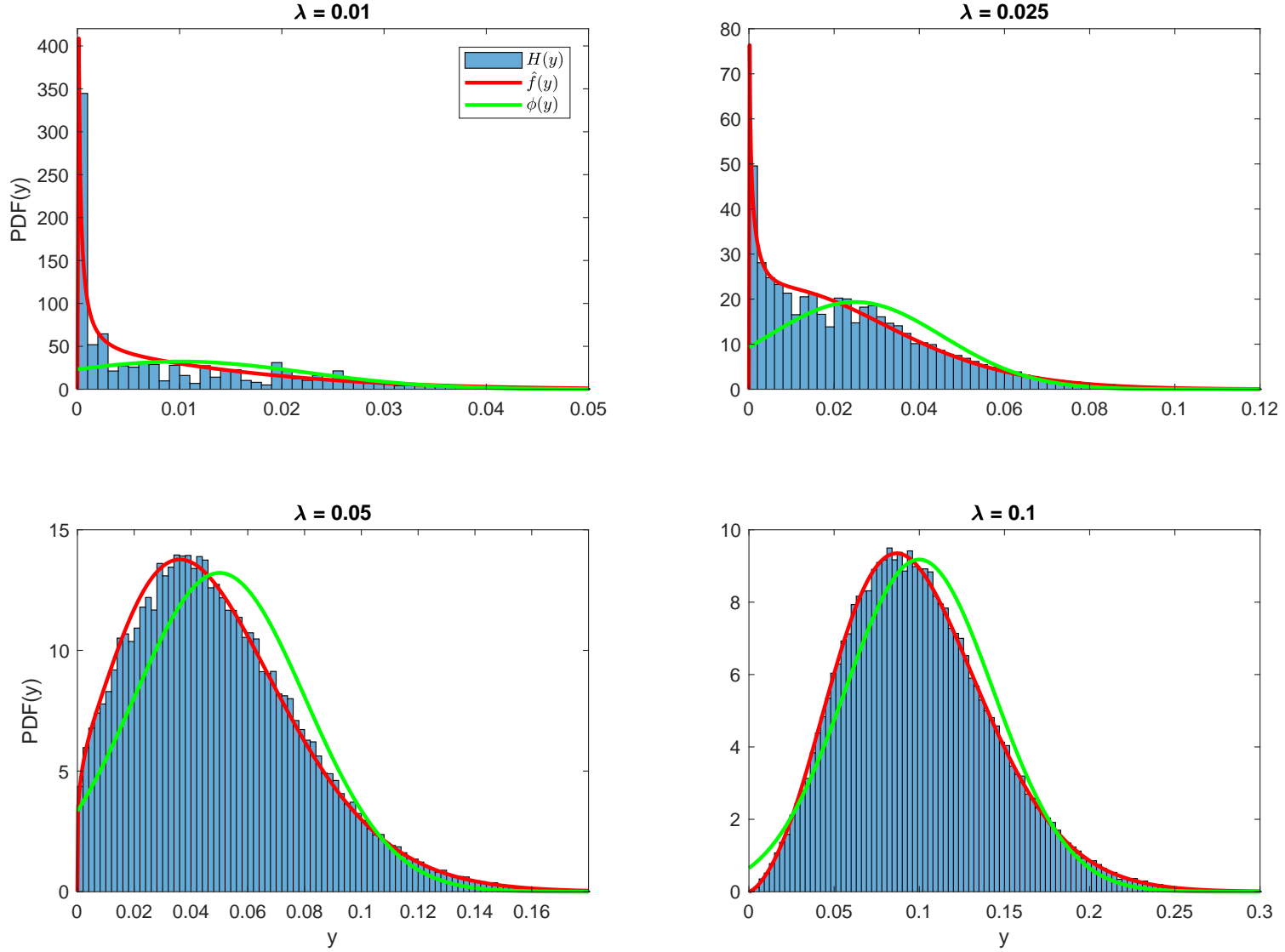


Fig. 1. PDF in the case of the saddlepoint approximation (red curve) and the best Gaussian fit (green curve) of the PDF of the statistic $y = T(\mathbf{x})$ vs. the corresponding histogram $H(y)$ obtained with a set of 10^5 MF filtered random realizations of a Poisson 13×13 pixels noise process with the parameter λ set to 0.01, 0.025, 0.05, and 0.1 counts pix^{-1} (see Sect.5 for details). The used MF is given by Eq. (5) with s a circular Gaussian with standard deviation $\sigma = 2$ pixels normalized to unit volume.

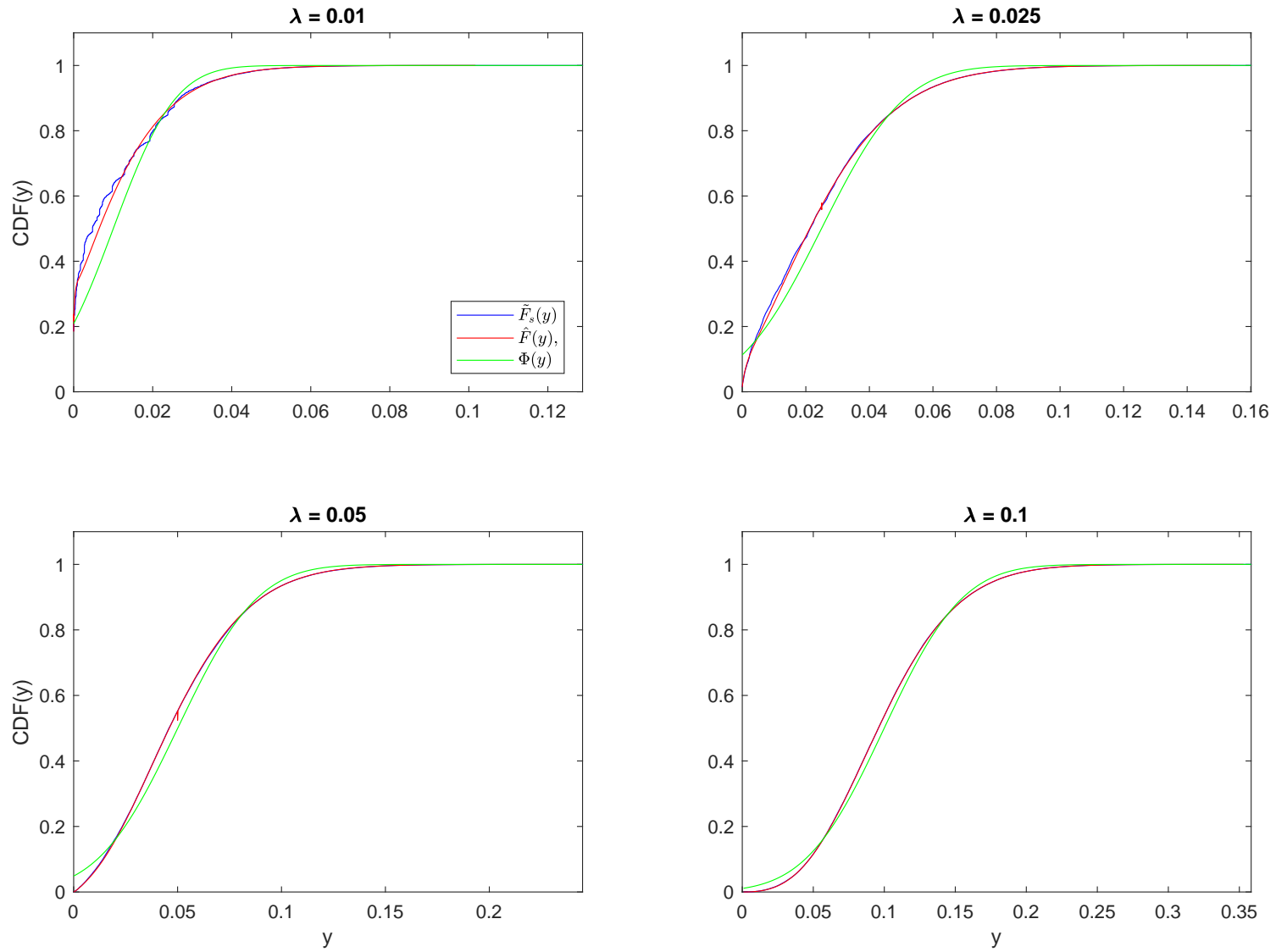


Fig. 2. CDFs corresponding to the the PDFs shown in Fig. 1. The saddlepoint approximation is drawn with a red line, the best Gaussian fit with a green line, and the sample CDF with a blue line.

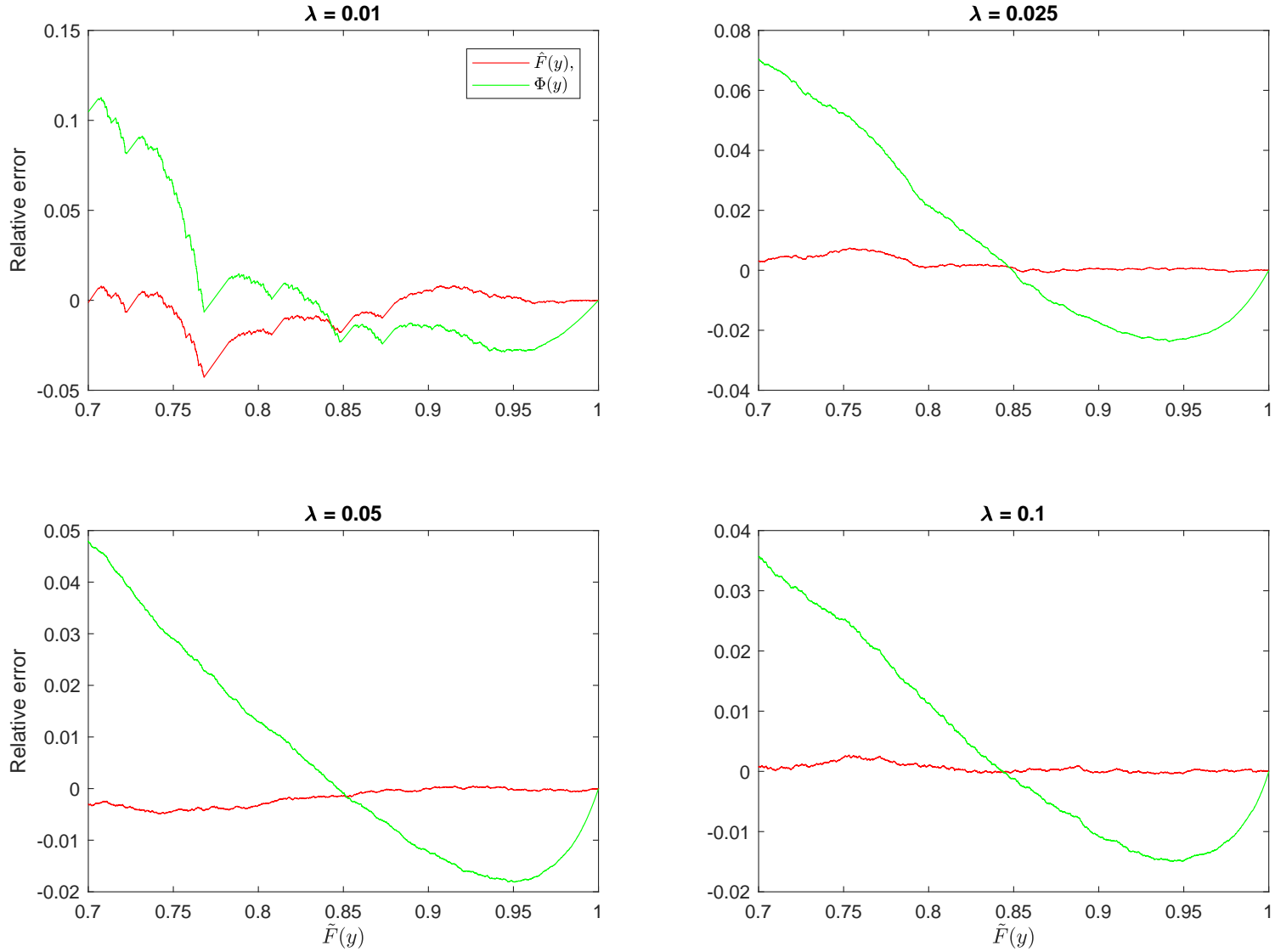


Fig. 3. Relative errors $(\hat{F}(y) - \tilde{F}(y))/\tilde{F}(y)$ (red line) and $(\Phi(y) - \tilde{F}(y))/\tilde{F}(y)$ (green line) against $\tilde{F}(y)$ for the CDF's in Fig. 2. The very small relative errors of $\tilde{F}(y)$ highlight its good performance. However, caution has to be used when considering the very right end of these diagrams. This is because $\tilde{F}(y)$ is not an accurate estimate of $F(y)$ when this last is very close to one. Indeed, $F(y) \rightarrow 1$ only when $y \rightarrow \infty$ but $\tilde{F}(y_{\max}) = 1$ with y_{\max} the greatest among the simulated random variable Y .

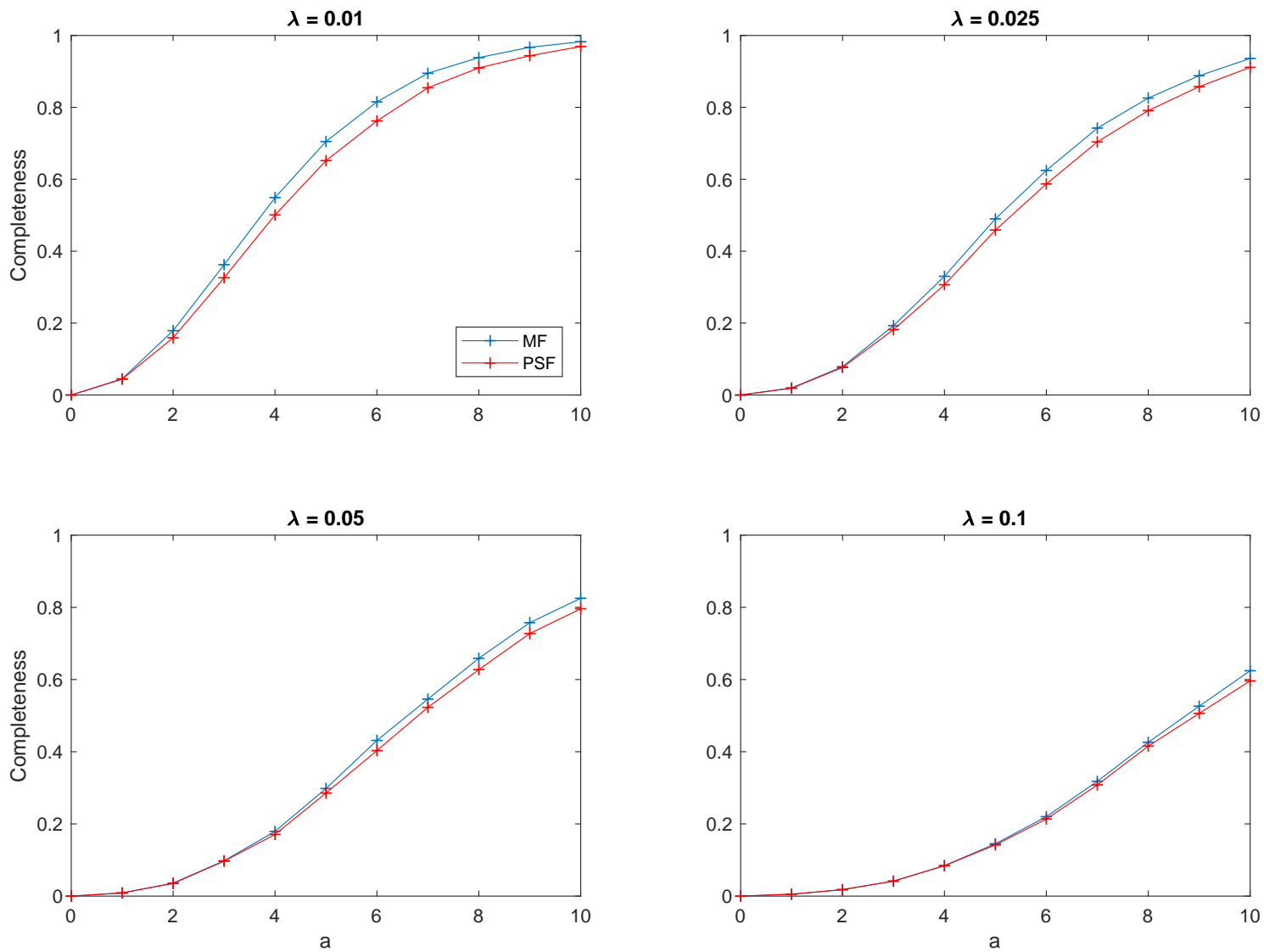


Fig. 4. Completeness (fraction of correctly detected signals) as function of their amplitude a for fixed values of the intensity λ (units in counts pix^{-1}) of the background. Here, the signal is given by ag with g a circular Gaussian with $\sigma = 2$ pixels and normalized to unit volume. 10^4 simulated 13×13 pixels maps have been used. The detection test has been run on the pixel corresponding to the position of the signal.

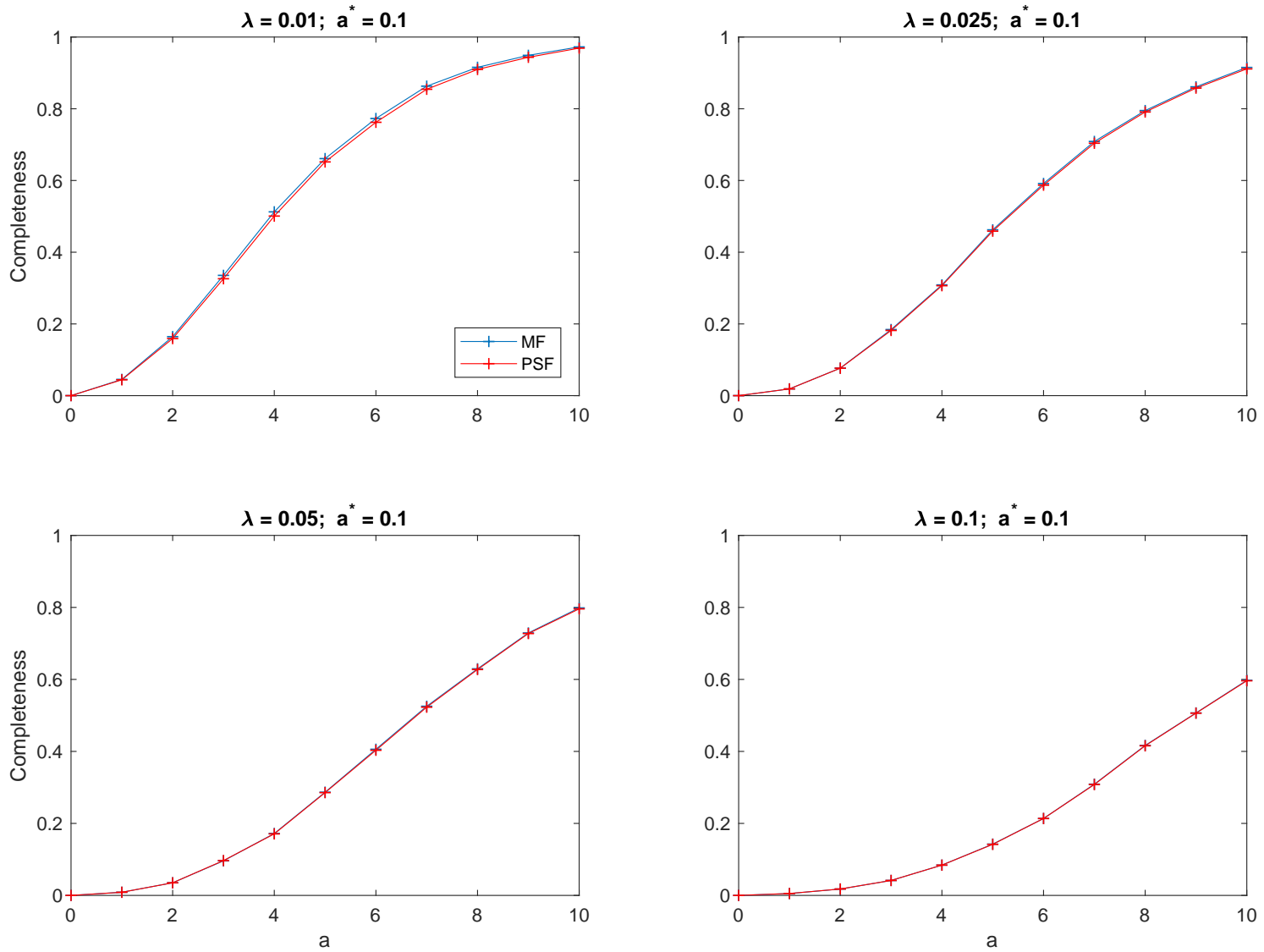


Fig. 5. As in Fig. 4 but the MF has been computed using an incorrect value $a^* = 0.1$ for the amplitude a of the signal.

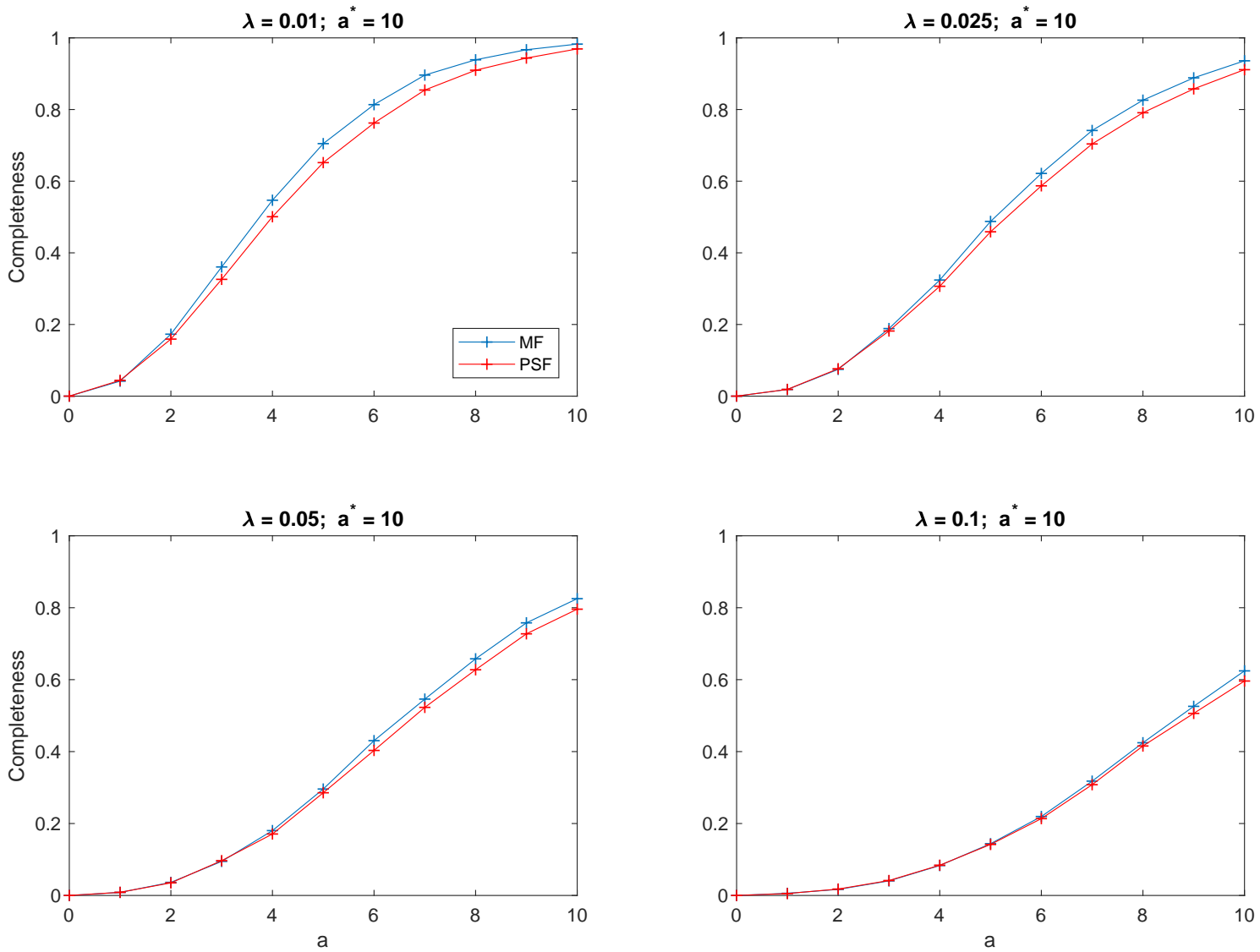


Fig. 6. As in Fig. 4 but the MF has been computed using an incorrect value $a^* = 10$ for the amplitude a of the signal.

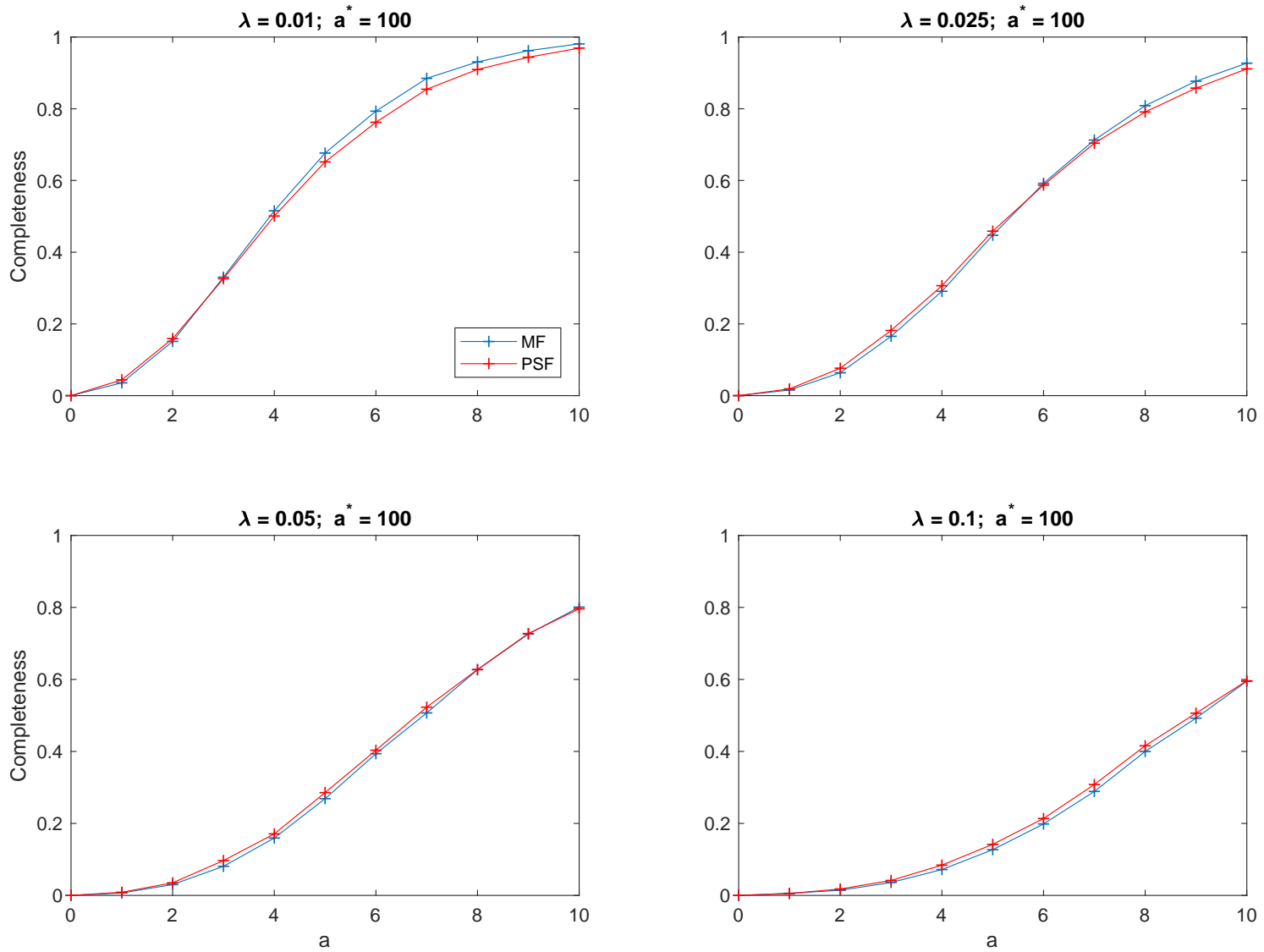


Fig. 7. As in Fig. 4 but the MF has been computed using an incorrect value $a^* = 100$ for the amplitude a of the signal.

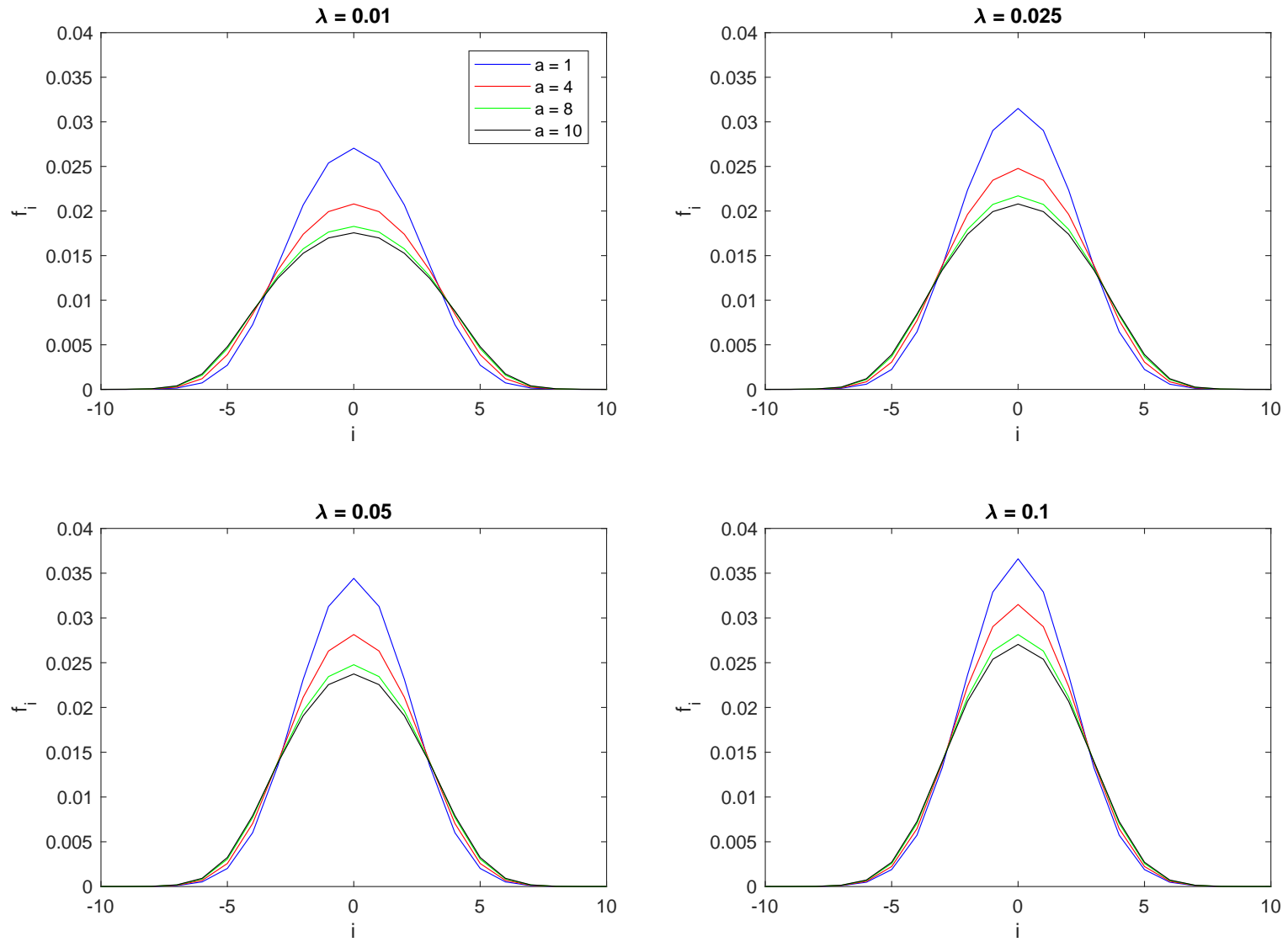


Fig. 8. 1-D cuts of the MF for different values of the amplitude a and fixed value of the intensity parameter λ of the background.

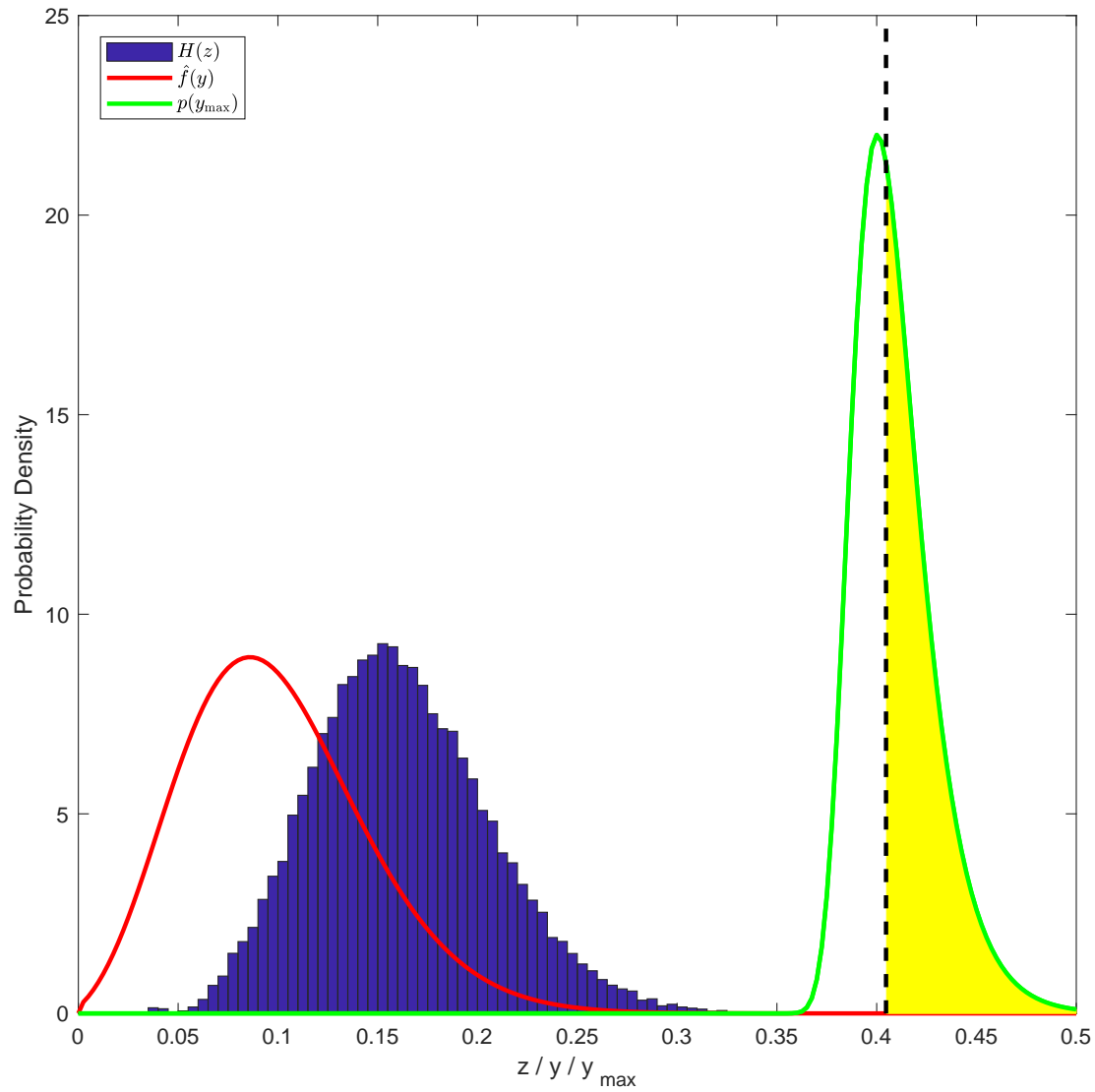


Fig. 9. Comparison of the saddlepoint approximation $\hat{f}(y)$ (red line) of the PDF of the counts of a MF filtered 2000×2000 pixels Poisson random field ($\lambda = 0.1$ counts pix^{-1}) with the histogram $H(z)$ of its peaks. The used MF is given by Eq. (5) with s a circular Gaussian with $\sigma = 2$ pixels and normalized to unit volume. For reference, the PDF $p(y_{\max})$ (green line) of the greatest value of the map is also drawn (see text). The color-filled area provides the SPFA for the greatest peak effectively observed in the simulated map (SPFA ≈ 0.47).